International Journal of Technology (2016) 1: 26-37
ISSN 2086-9614

VOLTAGE PROFILE IMPROVEMENT OF THE 20 KV PAINAN DISTRIBUTION SYSTEM WITH MULTIPLE DISTRIBUTED RENEWABLE ENERGY GENERATION

Refdinal Nazir[1*], Muhammad Nurdin[2], Eka Fitrianto[1]

[1] *Department of Electrical Engineering, Faculty of Engineering, Universitas Andalas, Limau Manis, Pauh, West Sumatera 25163, Indonesia*
[2] *School of Electrical Engineering and Informatics, Institut Teknologi Bandung, Jl. Ganesha 10, Bandung, Indonesia*

(Received: October 2015 / Revised: December 2015 / Accepted: January 2016)

ABSTRACT

This paper analyzes the effect of multiple Distributed Renewable Energy Generation penetration on improving the performance of the B3 feeder typical distribution system structure in Painan, Indonesia. Analysis uses a simple concept of load and distributed generation current injection at the distributed main, lateral and sublateral lines. The algorithm begins from completion of the main line variables, then uses an algorithm to complete the lateral line variables associated with the main line variable, and finally calls algorithms to resolve the sublateral variables associated with the lateral line variable. The results have shown that integrating three Distributed Renewable Energy Generation units to this distributed system has increased the minimum voltage of the main line from 17.35 kV to 20.37 kV, reduced active power loss from 1914.747 kW to 569.925 kW, and diminished reactive power loss from 650.747 kVAr to 188.624 kVAr.

Keywords: Distributed Renewable Energy Generation (DREG); Distribution System (DS); Voltage profile; Active power loss; Reactive power loss

1. INTRODUCTION

Currently, electrical power generation systems in all parts of the world are changing from large centralized power plants to small distributed power plants placed near the load, which is widely known as distributed generation (DG). The benefits of the DG on the electrical system is identified in several previous studies (Pathomthat & Ramakumar, 2004; Gopiya et al., 2012; Davda et al., 2011), to include: reduced losses, improved system reliability, reduced voltage drop, reduced need for reactive power and improved networking capabilities to deliver power. In addition, DG can be developed using local renewable energy sources, such as micro/mini hydro, solar energy, wind energy, biomass, etc. Selection of the type of renewable energy used for DG depends highly on the topology, location and climate of the area where it is placed.

The Indonesian government has been anticipating the development of Distributed Renewable Energy Generation (DREG) using environmentally friendly energy sources for local electrical energy supply. A number of government policies support the development of DREG through various ministerial regulations of energy and natural resources (Kementrian ESDM, 2009). In fact, the government's business plans include several small-scale hydropower facilities to drive

* Corresponding author's email: refdinalnazir@yahoo.co.id, Tel. +62-812-66558708, Fax. +62-751-72566
Permalink/DOI: http://dx.doi.org/10.14716/ijtech.v7i1.2193

DG in power supply development (PT PLN, 2015).

A view previous papers have discussed DG integration to a Distribution System (DS), analyzing power loss reduction (Dipak et al., 2015; Sampath & Inamdar, 2011) and determining the optimal placement location of DG (Sampath & Inamdar, 2011; Caisheng & Hashem, 2004). Some researchers have analyzed voltage increases in a simple two-bus radial distribution network and a distribution network (with and without DG) using a worst case scenario (Mahmud et al., 2011). The effects of integrating a mini-hydro power plant at the end of the radial distribution network are also discussed in Refdinal and Topan (2007). Some previous studies focused on one variable of distribution system performance, while other studies focused on one type of DG.

This paper discusses the effect of multiple DREG penetration on the performance improvement of the B3 feeder Painan distribution system with typical structure. B3 feeder is one of the feeder of DS Painan that supplies electric power to some subdistrict in the north of Pesisir Selatan district, Indonesia. T Three small-scale hydropower DREG units serve as the object of this study. Analysis is performed using the MATLAB computer program to solve three variables of DS performance: voltage profile, active power loss and reactive power consumptions. In this study,a simple method of injection currents at all nodes in the main, lateral and sublateral lines is applied to solve the research variables.

2. ANALYSIS OF THE INTEGRATION OF DG TO THE DS

2.1. Radial Distribution System without DG

A radial distribution system (RDS) has at least one main line and can be equipped with lateral and sublateral lines (Ramana et al., 2013). As shown in Figure 1a, the main line and the lateral line have *m* and *l* nodes respectively, while the sublateral line consists of node *s*. It is assumed that the lateral line branches off the main line on node 3, while the sublateral line is the branch off the lateral line at node 3_2. Electrical power for the RDS is supplied by one feeder at a substation and routed through a medium-voltage distribution network to load points.

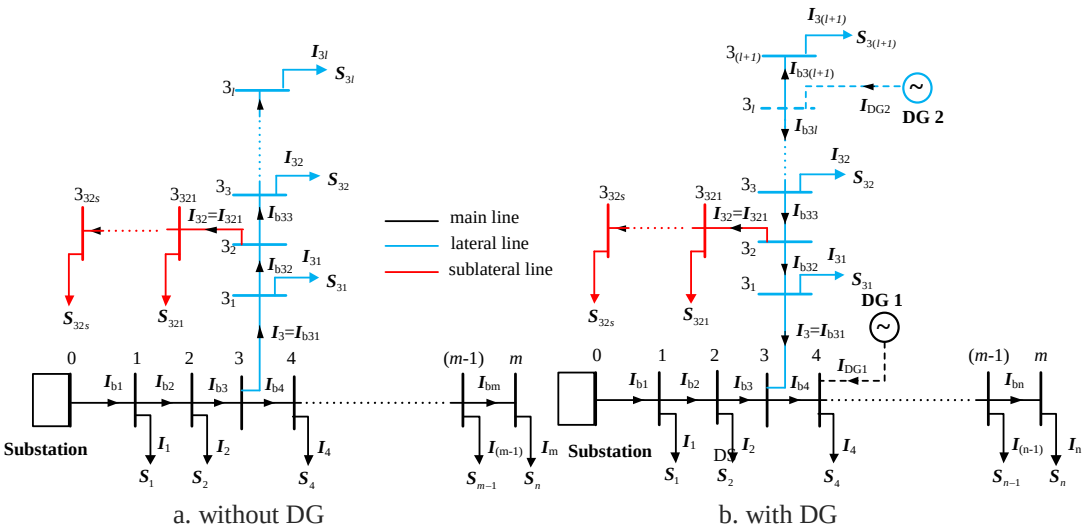

Figure 1 Single-line diagram of typical RDS structure

In this analysis, three-phase load (***S***) is assumed in delta connections and balanced conditions. The loads can be modeled as *constant active* and *reactive power* (PQ models) (Kersting, 2002). The DS complex power supplied to the load on node i is expressed by the following equation:

$$\boldsymbol{S}_i = \sqrt{3}\,\boldsymbol{V}_i\boldsymbol{I}_i^* = P_i + jQ_i \quad \text{for i =1,2,3,....}m \tag{1}$$

where P_i = three phase active power of load for ith node; Q_i = three phase reactive power of load for ith node; $\boldsymbol{V}_i$ = line to line voltage for ith node; $\boldsymbol{I}_i$ = load injection current for ith node.
From Equation 1, the load injection current at node i, $\boldsymbol{I}_i$, can be written as (Jen-Hao, 2003):

$$\boldsymbol{I}_i = \left(\frac{P_i + jQ_i}{\sqrt{3}\boldsymbol{V}_i} \right)^* \quad \text{for i=1,2,3,....}m \tag{2}$$

As shown in Figure 1a, node 3 of the main line is connected to the lateral line that contains *l* nodes. At this node, the load injection current on the main line can be solved by calculating the branch current of the lateral line, $\boldsymbol{I}_3 = \boldsymbol{I}_{b31}$. Likewise, the node 2 of the lateral line connected to the sublateral line that is constructed by *s* nodes. The injection current of lateral line at node of 2 is equal to the first branch current of sublateral, $\boldsymbol{I}_{32} = \boldsymbol{I}_{b321}$.

Referring to Figure 1a, the relationship between vector of branch current $[\boldsymbol{I}_b]$ and vector of load injection current $[\boldsymbol{I}]$ on the main line can be completed through the following equation:

$$\begin{bmatrix} \boldsymbol{I}_{b1} \\ \boldsymbol{I}_{b2} \\ \boldsymbol{I}_{b3} \\ \boldsymbol{I}_{b4} \\ \vdots \\ \boldsymbol{I}_{b(m-1)} \\ \boldsymbol{I}_{bm} \end{bmatrix} = \begin{bmatrix} 1 & 1 & 1 & 1 & \cdots & 1 & 1 \\ 0 & 1 & 1 & 1 & \cdots & 1 & 1 \\ 0 & 0 & 1 & 1 & \cdots & 1 & 1 \\ 0 & 0 & 0 & 1 & \cdots & 1 & 1 \\ \vdots & \vdots & \vdots & \vdots & \vdots & 1 & 1 \\ 0 & 0 & 0 & 0 & \cdots & 1 & 1 \\ 0 & 0 & 0 & 0 & \cdots & 0 & 1 \end{bmatrix} \begin{bmatrix} \boldsymbol{I}_1 \\ \boldsymbol{I}_2 \\ \boldsymbol{I}_3 \\ \boldsymbol{I}_4 \\ \vdots \\ \boldsymbol{I}_{(m-1)} \\ \boldsymbol{I}_m \end{bmatrix} \tag{3}$$

where $\boldsymbol{I}_{bj}$ is the current of branch between node j-1 and node j, $\boldsymbol{I}_j$ is the injection current of load for node j.

Referring to the source bus (node 0), the voltage at each node of the main line can be computedby the following equation:

$$\begin{bmatrix} \boldsymbol{V}_1 \\ \boldsymbol{V}_2 \\ \boldsymbol{V}_3 \\ \boldsymbol{V}_4 \\ \vdots \\ \boldsymbol{V}_{(m-1)} \\ \boldsymbol{V}_m \end{bmatrix} = \begin{bmatrix} \boldsymbol{V}_0 \\ \boldsymbol{V}_0 \\ \boldsymbol{V}_0 \\ \boldsymbol{V}_0 \\ \vdots \\ \boldsymbol{V}_0 \\ \boldsymbol{V}_0 \end{bmatrix} - \begin{bmatrix} \boldsymbol{Z}_{01} & 0 & 0 & 0 & \cdots & 0 & 0 \\ \boldsymbol{Z}_{01} & \boldsymbol{Z}_{12} & 0 & 0 & \cdots & 0 & 0 \\ \boldsymbol{Z}_{01} & \boldsymbol{Z}_{12} & \boldsymbol{Z}_{23} & 0 & \cdots & 0 & 0 \\ \boldsymbol{Z}_{01} & \boldsymbol{Z}_{12} & \boldsymbol{Z}_{23} & \boldsymbol{Z}_{34} & \cdots & 0 & 0 \\ \vdots & \vdots & \vdots & \vdots & \vdots & \vdots & \vdots \\ \boldsymbol{Z}_{01} & \boldsymbol{Z}_{12} & \boldsymbol{Z}_{23} & \boldsymbol{Z}_{34} & \cdots & \boldsymbol{Z}_{(m-2)(m-1)} & 0 \\ \boldsymbol{Z}_{01} & \boldsymbol{Z}_{12} & \boldsymbol{Z}_{23} & \boldsymbol{Z}_{34} & \cdots & \boldsymbol{Z}_{(m-2)(m-1)} & \boldsymbol{Z}_{(m-1)m} \end{bmatrix} \begin{bmatrix} \boldsymbol{I}_{b1} \\ \boldsymbol{I}_{b2} \\ \boldsymbol{I}_{b3} \\ \boldsymbol{I}_{b4} \\ \vdots \\ \boldsymbol{I}_{b(m-1)} \\ \boldsymbol{I}_{bm} \end{bmatrix} \tag{4}$$

where $\boldsymbol{V}_0$ is the voltage of source bus that defined the reference voltage, $\boldsymbol{V}_i$ is the voltage of node i, and $\boldsymbol{Z}_{ij}$ is the impedance between node i and node j of main line. Equation for the voltage drop can be solved from Equation 4, as follows:

$$[\Delta \boldsymbol{V}] = [\boldsymbol{Z}][\boldsymbol{I}_b] \tag{5}$$

where $[\Delta \boldsymbol{V}] = [\boldsymbol{V}_m - \boldsymbol{V}_0]$ is the vector of voltage drop for main line.
The power loss in the main line can be solved using the following equation:

$$P_{Loss} = real\left\{\sum_{i=1}^{m} 3\left|\boldsymbol{I}_{\mathrm{bi}}\right|^2 \boldsymbol{Z}_{(i-1)i}\right\} \tag{6a}$$

$$Q_{Loss} = imag\left\{\sum_{i=1}^{m} 3\left|\boldsymbol{I}_{\mathrm{bi}}\right|^2 \boldsymbol{Z}_{(i-1)i}\right\} \tag{6b}$$

Further, since node 3 of the main line is connected to the lateral line, the load injection current node 3, $\boldsymbol{I}_3$, is same the current branch between nodes 3_0 and node 3_1 on the lateral line, $\boldsymbol{I}_{\mathrm{b31,}}$ or $\boldsymbol{I}_3 = \boldsymbol{I}_{\mathrm{b31}}$. The branch current on the lateral line for each node can be solved using the following equation:

$$\begin{bmatrix} \boldsymbol{I}_{b31} \\ \boldsymbol{I}_{b32} \\ \boldsymbol{I}_{b33} \\ \square \\ \boldsymbol{I}_{b3l} \end{bmatrix} = \begin{bmatrix} 1 & 1 & 1 & \square & 1 \\ 0 & 1 & 1 & \square & 1 \\ 0 & 0 & 1 & \square & 1 \\ \square & \square & \square & \square & \square \\ 0 & 0 & 0 & \square & 1 \end{bmatrix} \begin{bmatrix} \boldsymbol{I}_{31} \\ \boldsymbol{I}_{32} \\ \boldsymbol{I}_{33} \\ \square \\ \boldsymbol{I}_{3l} \end{bmatrix} \tag{7}$$

The load injection current and voltage drop for each node on lateral line is solved using Equation 2 and Equation 5, respectively. Meanwhile, the power loss in the lateral line is determined using Equations 6a and 6b.

As illustrated by the structure of DS in Figure 1a, the lateral line is also connected with sublateral line on node 3_2, then the current $\boldsymbol{I}_{32}$ in the lateral line not from Equation 7, but is determined from the first branch current of sublateral line $\boldsymbol{I}_{321}$ (see Figure 1a). Furthermore, the stages of calculations performed for the sublateral line are similar to the steps for calculating the lateral line.

2.2. Radial Distribution System with DG

Integration of the RDG on the DS can be accomplished on the main, lateral and sublateral lines. In this analysis, the DERG energy sources used small-scale hydropower located throughout the DS. Assuming that the integration of RDG on DS can be carried either on the main or lateral line, as shown in Figure 1b, the integration of DG can be carried out directly on the existing node or the new node. The DG can also be modeled on the constant PQ model (Sivkumar et al., 2014), but with the direction of DG injection current opposite to the load injection current (see Figure 1b).

For the first case, the integration of DG1 on DS is performed directly on node 4 of the main line. This integration does not change the number of nodes on the main line, but it will change the current value of the branch at nodes 1, 2, 3 and 4. In this case, the calculation of the current branch is accomplished by substituting the current $\boldsymbol{I}_{\mathrm{DG1}}$ in Equation 3 to obtain the following equation:

$$\begin{bmatrix} \boldsymbol{I}_{b1} \\ \boldsymbol{I}_{b2} \\ \boldsymbol{I}_{b3} \\ \boldsymbol{I}_{b4} \\ \square \\ \boldsymbol{I}_{b(m-1)} \\ \boldsymbol{I}_{bm} \end{bmatrix} = \begin{bmatrix} 1 & 1 & 1 & 1 & \square & 1 & 1 \\ 0 & 1 & 1 & 1 & \square & 1 & 1 \\ 0 & 0 & 1 & 1 & \square & 1 & 1 \\ 0 & 0 & 0 & 1 & \square & 1 & 1 \\ \square & \square & \square & \square & \square & 1 & 1 \\ 0 & 0 & 0 & 0 & \square & 1 & 1 \\ 0 & 0 & 0 & 0 & \square & 0 & 1 \end{bmatrix} \begin{bmatrix} \boldsymbol{I}_1 \\ \boldsymbol{I}_2 \\ \boldsymbol{I}_3 \\ \boldsymbol{I}_4 - \boldsymbol{I}_{\mathrm{DG1}} \\ \square \\ \boldsymbol{I}_{(m-1)} \\ \boldsymbol{I}_m \end{bmatrix} \tag{8}$$

The value of DG1 current injected into the DS, $\boldsymbol{I}_{\mathrm{DG1}}$, can be written as:

$$\boldsymbol{I}_{\mathrm{DG1}} = \left(\frac{\boldsymbol{S}_{DG1}}{\sqrt{3}\boldsymbol{V}_4} \right)^* = \left(\frac{P_{\mathrm{DG1}} + jQ_{\mathrm{DG1}}}{\sqrt{3}\boldsymbol{V}_4} \right)^* \tag{9}$$

where P_{DG1} and Q_{DG1} is active and reactive power supplied by DG.

The change of branch current in the main line will affect the voltage drop on each node and power losses in the main line.

Unlike the first case, the integration of DG_2 on DS will cause an increase in the number of nodes on the lateral line into $l + 1$, changing the current equation in the lateral branch line to:

$$\begin{bmatrix} \boldsymbol{I}_{b31} \\ \boldsymbol{I}_{b32} \\ \boldsymbol{I}_{b33} \\ \vdots \\ \boldsymbol{I}_{b3l} \\ \boldsymbol{I}_{b3(l+1)} \end{bmatrix} = \begin{bmatrix} 1 & 1 & 1 & \cdots & 1 & 1 \\ 0 & 1 & 1 & \cdots & 1 & 1 \\ 0 & 0 & 1 & \cdots & 1 & 1 \\ \vdots & \vdots & \vdots & \vdots & \vdots & \vdots \\ 0 & 0 & 0 & \cdots & 1 & 1 \\ 0 & 0 & 0 & \cdots & 0 & 1 \end{bmatrix} \begin{bmatrix} \boldsymbol{I}_{31} \\ \boldsymbol{I}_{32} \\ \boldsymbol{I}_{31} \\ \vdots \\ -\boldsymbol{I}_{\mathrm{DG}2} \\ \boldsymbol{I}_{3(l+1)} \end{bmatrix} \tag{10}$$

The value of DG2 current injected into DS ($\boldsymbol{I}_{\mathrm{DG2}}$) can be solved using Equation 9, with $\boldsymbol{V}_4$ replaced by $\boldsymbol{V}_{3l}$.

3. CASE STUDY

This research examines the 20 kV Painan DS in West Sumatra, Indonesia. In this DS, the electrical power is supplied by a 30 MVA Bungus substation through 20 kV lines, as shown in Figure 2. The maximum load reaches 11.8 MW, which is spread across six load points (sub DS) and is supplied through two main feeders (B3 and PN). In this case, the B3 feeder supplies electrical power to B3, TR and PB sub DS. Meanwhile, the load on the PN sub DS is separated into two parts (PN1 and PN2), where the load on PN1 and PN2 is supplied by the B3 feeder and PN feeder respectively. At this time, Painan DS has also integrated a 0.7 MW Mini Hydro Power Plant (MHPP) as DG at PN1. A typical structure of sub DS in B3 feeder are shown in detail in Appendix 2.

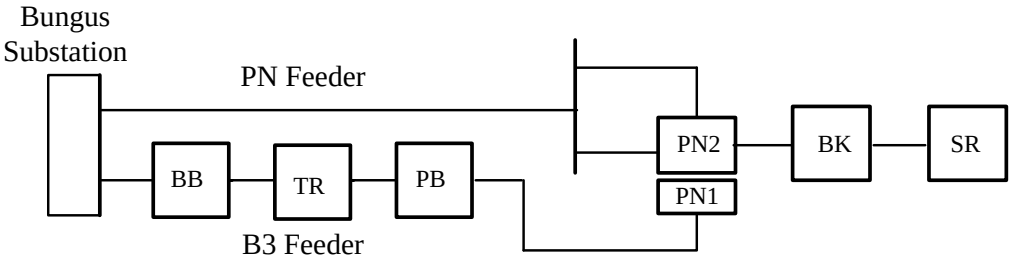

Figure 2 Typical structure of Painan DS applied as case study

Table 1 presents B3 feeder parameters for each sub DS. The number of lateral, sublateral and node reached 21, 18 and 170 respectively. The PB sub DS contains the largest number of nodes. The length of line between nodes that are used to calculate the line impedance has been obtained from the mapping of DS using GPS, while the load data has been obtained from the measurement of transformer loading in the 1st quarter 2015 by the National Electricity Company (PLN). In this DS, all lines use A3C conductors with a 150 mm^2 cross section. In addition, the length of the main line for the B3 feeder achieves 59.90 km and the DS power factor is 0.8.

Table 1 B3 feeder parameters

Subdistrict	Amount of		
	Lateral	Sublateral	Node
BB	1	0	18
TR	5	3	38
PB	6	9	76
PN1	9	18	38
Total	21	18	170

In the study area, there are a number of small-scale hydropower units that can be developed into MHPP as DG. Some of these energy resources have been investigated in terms of feasibility and are already included in the PLN electricity supply development plan (PLN, 2015). In this study, three MHPPs were integrated into the Painan district DS B3 feeder as DG to improve performance. Based on potential available location, three MHPP units were injected into the DS on two lateral lines (lateral nodes 39 and 64). Data of the DGs integrated into this DS are presented in Table 2.

Table 2 DC data

Name	Capacity	Location		Status
		Coordinates	at B3 feeder	
Salido Kecil (DG1)	0.7 MW	100^{0}38'25"E; 0101'38"S	64th Lateral, Node 9	Operating
Kerambil (DG2)	1.4 MW	100^{0}36'45"E; 01^{0}09'24"S	39th Lateral, Node 23	In Planning
Bayang (DG3)	4.5 MW	100^{0}37'37"E; 01^{0}11'28"S	39th Lateral, Node 21	In Planning

4. COMPUTER SIMULATION

In this study, analysis was performed using the MATLAB ver. R2012bv computer program. The design was based on the flowchart shown in Appendix 1. Referring to the typical structure of the DS, this flowchart is prepared on a flowchart for the main line, lateral line, and sublateral line. The flowchart of the main line includes the steps taken to resolve node voltages, branch currents and losses in the main line. The analytic process was repeated in several iterations (k), so node voltage changes on the main line had very small values ($\varepsilon=10^{-4}$). If a node of the main line had a lateral line, then the flowchart of lateral line was invoked through the command *function* to complete the current value of the lateral line that was injected into the main line.

Analysis of the lateral line is needed to calculate the value of current injected by the lateral line to the main line, as shown in Appendix 1. To begin the analysis of the lateral line, several variables and constants of the main program are called, which includes: a voltage node of the main line which was used as the reference voltage of the lateral line ($\boldsymbol{V}_{l0}$), the number of nodes for the lateral line (l) and impedance and power load of the lateral line ($\boldsymbol{Z}_l$ and $\boldsymbol{S}_l$). The calculated result of branch current and power losses on the lateral line was returned to the subsequent calculation of the main line. If a node of the lateral line contained a sublateral line, then the flowchart of the sublateral line was called through the function command to solve the current value of the sublateral line that injected into the lateral line. In this analysis, the computer simulation was conducted in four scenarios, as shown in Table 3.

Table 3 Simulation scenario

Simulation Scenario	DG Integrated			Comment
	DG1	DG2	DG3	
Scenario 1				without DG
Scenario 2	✓			with one unit
Scenario 3	✓	✓		with two units
Scenario 4	✓	✓	✓	with three

5. RESULTS

5.1. The Effect of DG Integration on DS against the Voltage Profile

The analysis results of DG integration on the B3 feeder in the Painan DS against the main line voltage profile is shown in Figure 3. For scenario 1 (without DG), the node voltage of the main line decreased rapidly by increasing the node distance from the substation (node 0). Above node 8, the node voltage dropped below the allowable standard value (19 kV). The integration of 0.7 MW DG at location 1 into this DS (scenario 2) increased the minimum node voltage from 17.35 kV to 17.82 kV. Furthermore, the integration of 0.7 and 1.4 MW DG respectively provided a better profile of the main line voltage, although there were still many below-standard voltage values. Meanwhile, the addition of 4.5 MW DG (scenario 4) raised all node voltages to exceed the voltage of node 0 (20.37kV).

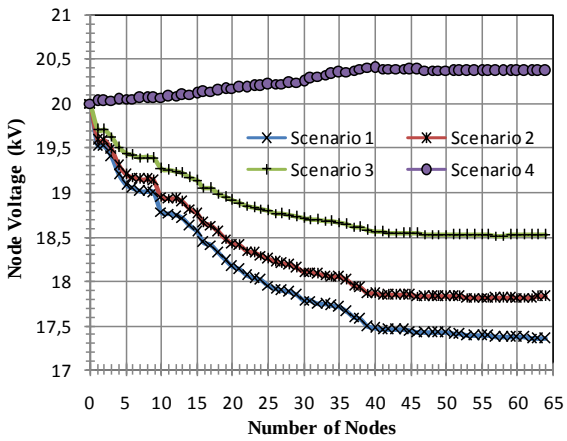

Figure 3 Effect on main line node voltage

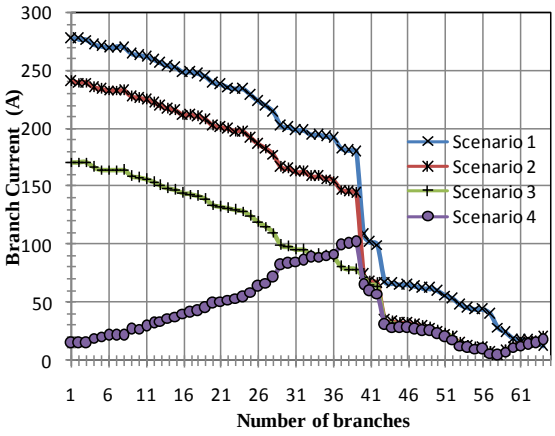

Figure 4 Effect on main line branch current

5.2. The Effect of DG Integration on DS against the Branch Current

As shown in Figure 4, the integration of DG on the B3 feeder in Painan DS decreased the maximum branch current values on the main line significantly, from 277.02 A (scenario 1) to 101.58 A (scenario 4). For scenarios 1, 2 and 3, the current branch between nodes decreased due to the increasing distance from the branch to the reference node (node 0). But for scenario 4, the current increased at the branches located before node 39, then the current decreased at the branches located after node 39. This may have occurred because the power injected by the DG to this DS is relatively large, so the current reverses direction at the branches located before node 39.

On the lateral line containing DG (lateral line of nodes 39 and 64), the branch current of the lateral line increased following the integration of DG on the DS, as shown in Figure 5. At the lateral line of node 64, there is only one unit of 0.7 MW DG at location 1. As shown in Figure 5b, the integration of DG on the DS at this location for scenarios 2, 3 and 4 has similar increases in branch current. There were two planned DG locations at the lateral line of node 39,

namely: 1.4 MW on location 2 and 4.5 MW at location 3. As shown in Figure 5a, the integration of all DG units in the DS (scenario 4) will increase the large branch current on the lateral line of node 39.

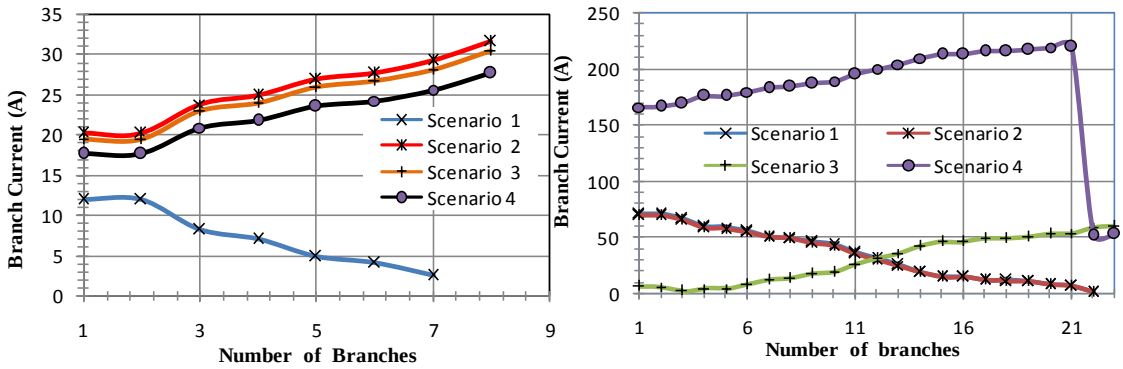

(a) lateral line of node 39 (b) lateral line of node 64

Figure 5 Effect of DG integration on lateral line branch current

5.3. The Effect of DG Integration on DS against Line Power Loss

As shown in Table 4, without DG penetration, the DS generated both active and reactive power losses reaching 1,914.747 kW and 650.747 kVAr, respectively. With the integration of 0.7 MW DG on the DS at lateral line node 64, active and reactive power losses dropped to 1389.374 kW and 472.583 kVAr. If the penetration of 1.4 MW DG and 4.5 MW DG at lateral line node 39 is accomplished in the DS, then the active and reactive power losses can be reduced to 569.925 kW and 188.624 kVAr, respectively.

Table 4 DS active and reactive power loss

Line	Active Power Losses (kW)				Reactive Power Losses (kVAr)			
	Scen. 1	Scen. 2	Scen. 3	Scen. 4	Scen.1	Scen. 2	Scen. 3	Scen. 4
Main Line	1,887.627	1,360.300	634.963	83.503	641.544	462.744	216.413	27.607
26th Lateral Line	0.010	0.016	0.015	0.013	0.013	0.015	0.014	0.012
28th Lateral Line	0.523	0.505	0.475	0.390	0.187	0.180	0.170	0.139
39th Lateral Line	19.004	18.198	22.536	477.698	6.286	6.020	7.561	157.962
42th Lateral Line	7.141	6.830	6.320	5.220	2.557	2.446	2.263	1.869
64th Lateral Line	0.442	3.525	3.265	3.101	0.160	1.178	1.091	1.035
Total	1,914.747	1,389.374	667.574	569.925	650.747	472.583	227.512	188.624

6. DISCUSSION

The effects of DG integration on DS performance depends on several factors, including DS structure, DG placement, number or size of DG units, etc. (Mahmud et al., 2011; Gopiya et al., 2012; Caisheng & Hashem, 2004). The integration of multiple RDGs to the B3 feeder in the Painan DS provided a positive impact on voltage and current profiles, and active and reactive power losses, as presented in sections 5.1, 5.2 and 5.3. Without DG (scenario 1), all DS branch current of the main, lateral and the sublateral lines flowed from the substation to the point of load or node. A high branch current magnitude and long main line distances trigger a large voltage decrease in the node, also causing greater active and reactive power loss in the main line.

When DG1 was integrated into the DS at lateral line node 64 (scenario 2), the lateral line and branch current of the main line after node 58 reverses direction, because of the injection current of DG1 at the end of the lateral line. This caused a reduction in the current flowing from the

substation to the point of load or node on the main line, a voltage drop or increase in the voltage node, and a reduction in active and reactive power loss from the main line. Almost all of the current branches of lateral line node 39 also reversed because of the integration of DG1 and DG2 at lateral line nodes 64 and 39 (scenario 3). This exacerbated current decline in the main line. Further, this also increased node voltage and reduced power loss in the main line.

When DG3 was integrated into the DS at lateral line node 39 (scenario 4), all main line branch currents before node 39 declined significantly and turned toward the substation. This may have occuroccurred due to the excess power of DG2 and DG3 that propagated from lateral line node 39 to the main line. This condition caused an increase in main line voltage above the referenced node voltage below node 39, and slightly fell above node 39 (see Figure 3). Also, main line power loss was reduced significantly, as was the lateral line power loss as node 39 increased. However, because the lateral line was much shorter than the main line, the increase of power losses in the lateral line was very small compared to the reduction of power losses in the main line (see Table 4)

7. CONCLUSION

In this paper, the effects of DG integration on the performance of the B3 feeder in the Painan DS have been successfully analyzed using a computer program. In general, the results have shown that DG integration into this DS has reduced line current, reversed the direction of line current, raised node voltage, and reduced both active and reactive power loss. The application of scenario 4 in this analysis provided the best performance of this DS, as indicated by the increase in main line minimum voltage from 17.35 kV to 20.37 kV, reduction in active power loss from 1914.747 kW to 569.925 kW, and decrease in the reactive power loss of 650.747 kVAr to 188.624 kVAr. Overall, it can be concluded that utilization of local renewable energy (i.e., small-scale hydropower) to drive DG can improve the performance of this DS and reduce the cost of development to cope with future load growth.

8. ACKNOWLEDGEMENT

The author would like thank the Engineering Faculty, Andalas University for the financial support of this work through Biaya Operasional Penguruan Tinggi (BOPT) Funding (No. 028/UN16/PL/AKS /2015).

9. REFERENCES

Caisheng, W., Hashem, N., 2004. Analytical Approaches for Optimal Placement of Distributed Generation Sources in Power System. *IEEE Transactions on Power Systems*, Volume 19(4), pp. 2068–2076

Davda, A.T., Desai, M.D., Parekh, B.R., 2011. Integration of Renewable Distributed Generation in Distribution System for Loss Reduction: A Case Study. *International Journal of Computer and Electrical Engineering*, Volume 3(3), pp. 413–416

Dipak, R.G., Chinala, Mallareddy, 2015. Optimal Placement of Distributed Generation for Loss Reduction in Distribution System by using Newton-Raphson Method. In: *the Proceedings of the 29th International Road Federation (IRF) Conference*, Pune, 21 June, India

Gopiya, N.S., Khatod, D.K., Sharma, M.P., 2012. Distributed Generation Impact on Distribution Networks: A Review. *IJEEE*, Volume 2(1), pp. 68–72

Jen-Hao, T., 2003. A Direct Approach for Distribution System Load Flow Solutions. *IEEE Transaction on Power Delivery*, Volume. 18(3), pp. 882–887

Kementrian ESDM, 2009. Peraturan Menteri Energi dan Sumber Daya Mineral Nomor 31 Tahun 2009, 13 November, pp. 2–3 (in Bahasa)

Kersting, W.H., 2002. *Distribution System Modeling and Analysis*. First Edition, New York: CRC Press LLC

Mahmud, M.A., Hossain, M.J., Pota, H.R., 2011. Analysis of Voltage Rise Effect on Distribution Network with Distributed Generation. In: *the Proceedings of the 18th International Federation of Automatic Control (IFAC) World Congress*, Milano, 28 August, Italy pp. 14796–14801

Pathomthat, Ch., Ramakumar, R., 2004. An Approach to Quantify the Technical Benefit of Distributed Generation. *IEEE Transactions on Energy Conversion*, Volume 19(4), pp. 764–773

PT PLN Persero, 2015. Rencana Usaha Penyediaan Tenaga Listrik (RUPTL) PT. PLN (Persero), 2015-2024, 12 January, pp. 217–222 (in Bahasa)

Ramana, T., Ganesh, V., Sivanagaraju, S., 2013. Simple and Fast Load Flow Solution for Electrical Power Distribution Systems. *International Journal on Electrical Engineering and Informatics (IJEEI)*, Volume 5(3), pp. 245–255

Refdinal, N., Topan, A., 2007. Analisis Manfaat Teknis Pengintegrasian PLTM Tersebar pada Sistem Distribusi. In: *the Proceedings of the Applied Technology, Science, and Arts (APTECS)*, 22 December, Surabaya, Indonesia (in Bahasa)

Sampath, K.B., Inamdar, H.P., 2011. Loss Reduction by Optimal Placement of Distributed Generation on a Radial Feeder. *International Journal on Electrical and Power Engineering*, Volume 02(01), pp. 24–29

Sivkumar, M., Debapriya, D., Subrata, P., 2014. A Simple Algorithm for Distribution System Load Flow with Distributed Generation. In: *the Proceeding of IEEE International Conference on Recent Advances and Innovations in Engineering (ICRAIE)*, 09-11 May, India

Appendix 1 Computer simulation flowchart

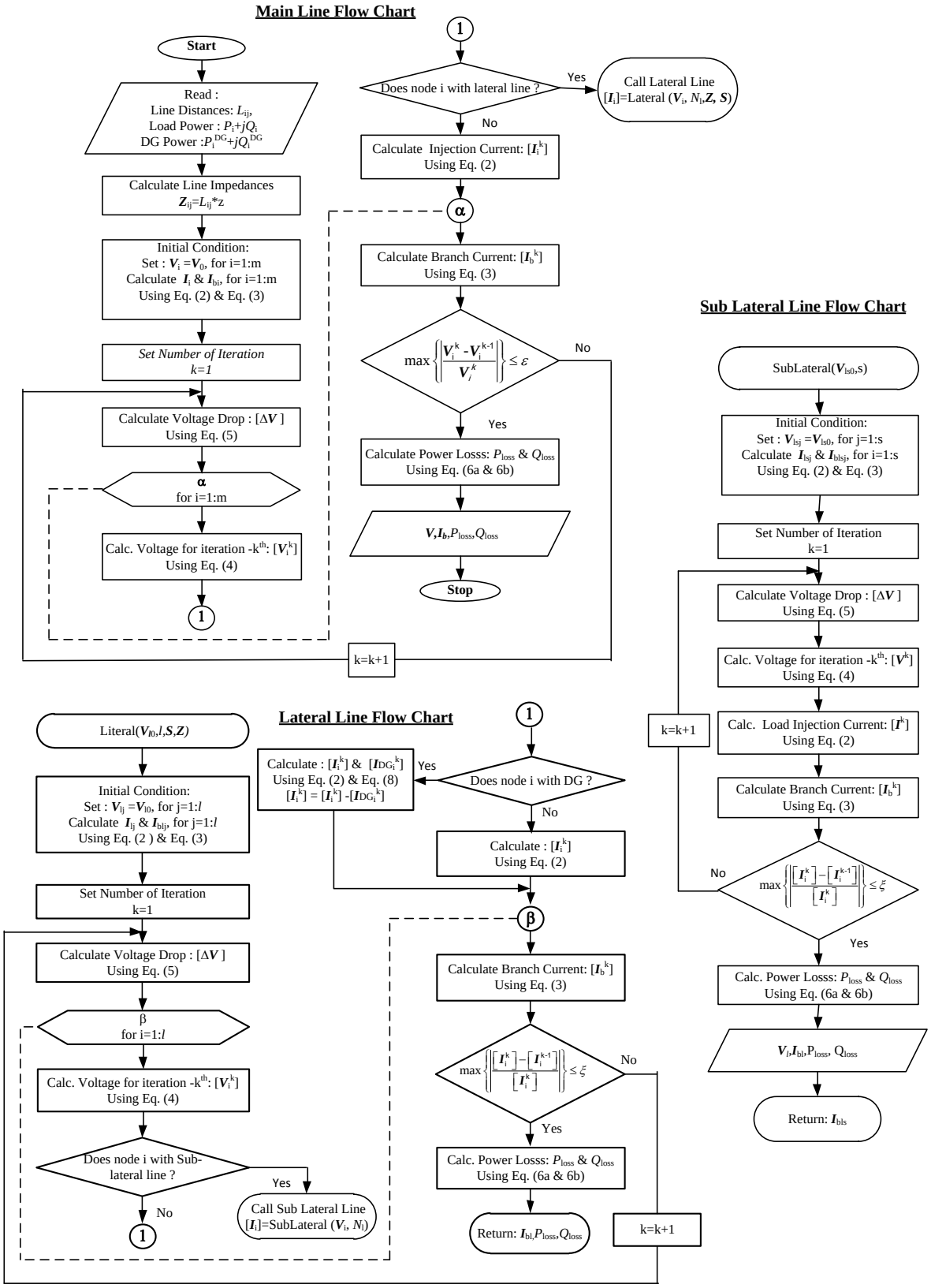

Appendix 2 B3 feeder of Painan DS networks